

Fig. S1. Identification and characterization of *Pcl*^{3-78*38}. (A) Deficiency mapping of 3-78 uncovered three lethal mutations (arrowheads) on chromosome 2R distal to *FRT42D* in regions 43A4-43D3, 50A1-50A7, and 55B5-55C2. The asterisk indicates the location of 3-78*38. (B-D) Unlike 3-78*56 (B), *Pcl*^{3-78*38} ELF mosaics (C) showed large Fas3-positive NE cell clusters (red, arrowheads). Smaller clusters were detected within the OPC (C, arrow). Targeting of R-cell axons labeled with mAB24B10 (red) and *ro- τ -lacZ* (blue) was largely normal (D). Brackets indicate the position of the lamina plexus containing R1-R6 growth cones. (E,F) *Pcl*^{2777a} ELF mosaics showed large (arrowheads) and small (arrow) Fas3-positive NE cell clusters at the third instar larval stage (E), that persisted into adulthood (F, arrowheads). (G) Strategy to distinguish NE cells and Nbs in the OPC. *neur*^{P72}-*Gal4* UAS-*cd8GFP* (green; white in inset) is expressed in Nbs (labeled by *Ase*, blue) and their progeny but not in NE cells and LPCs (outlined). La, lamina; Me, medulla; In, lamina neurons, LPC, lamina precursor cells. For genotypes and sample numbers, see Table S2. Related to Figs. 1,2. Scale bars: 50 μ m.

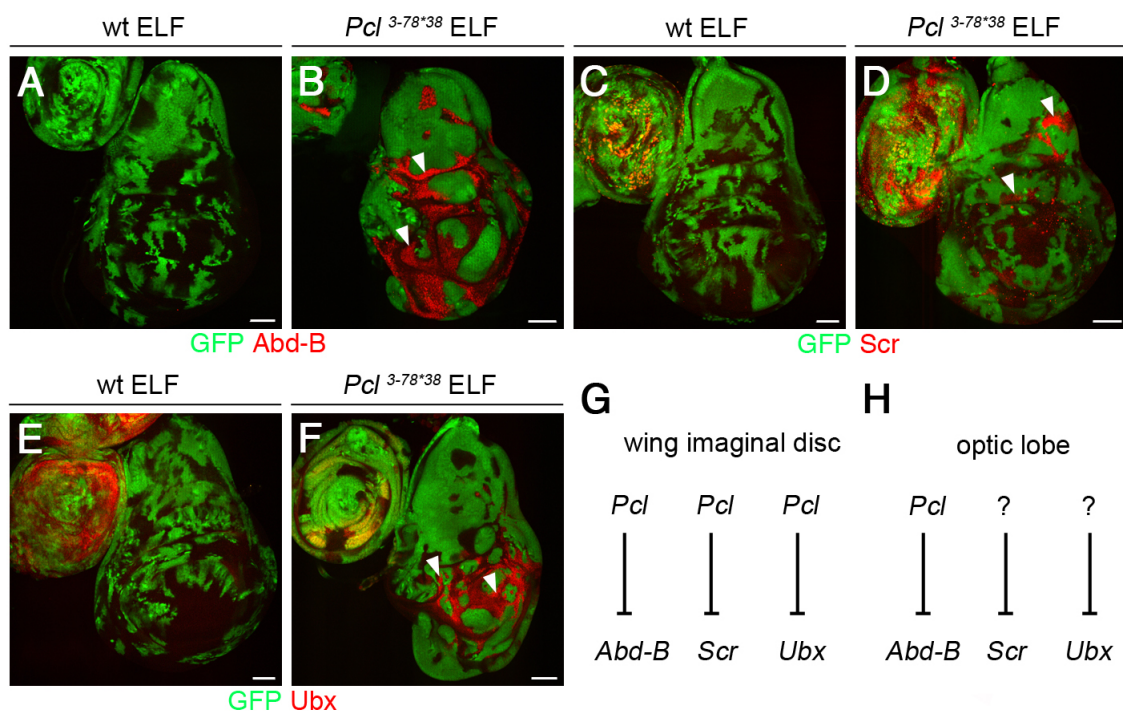


Fig. S2. *Pcl* represses *Hox* gene expression in wing imaginal discs. (A-F) Unlike controls (A,C,E), *Pcl*^{3-78*38} ELF mosaics showed ectopic *Abd-B* (red; B), *Scr* (red; D) and *Ubx* (red; F) expression in wing imaginal discs (arrowheads). (G,H) Model for differential regulation of *Hox* gene repression in wing imaginal discs (G) and optic lobes (H). For genotypes and sample numbers, see **Table S2**. Related to **Fig. 3**. Scale bars: 50 μ m.

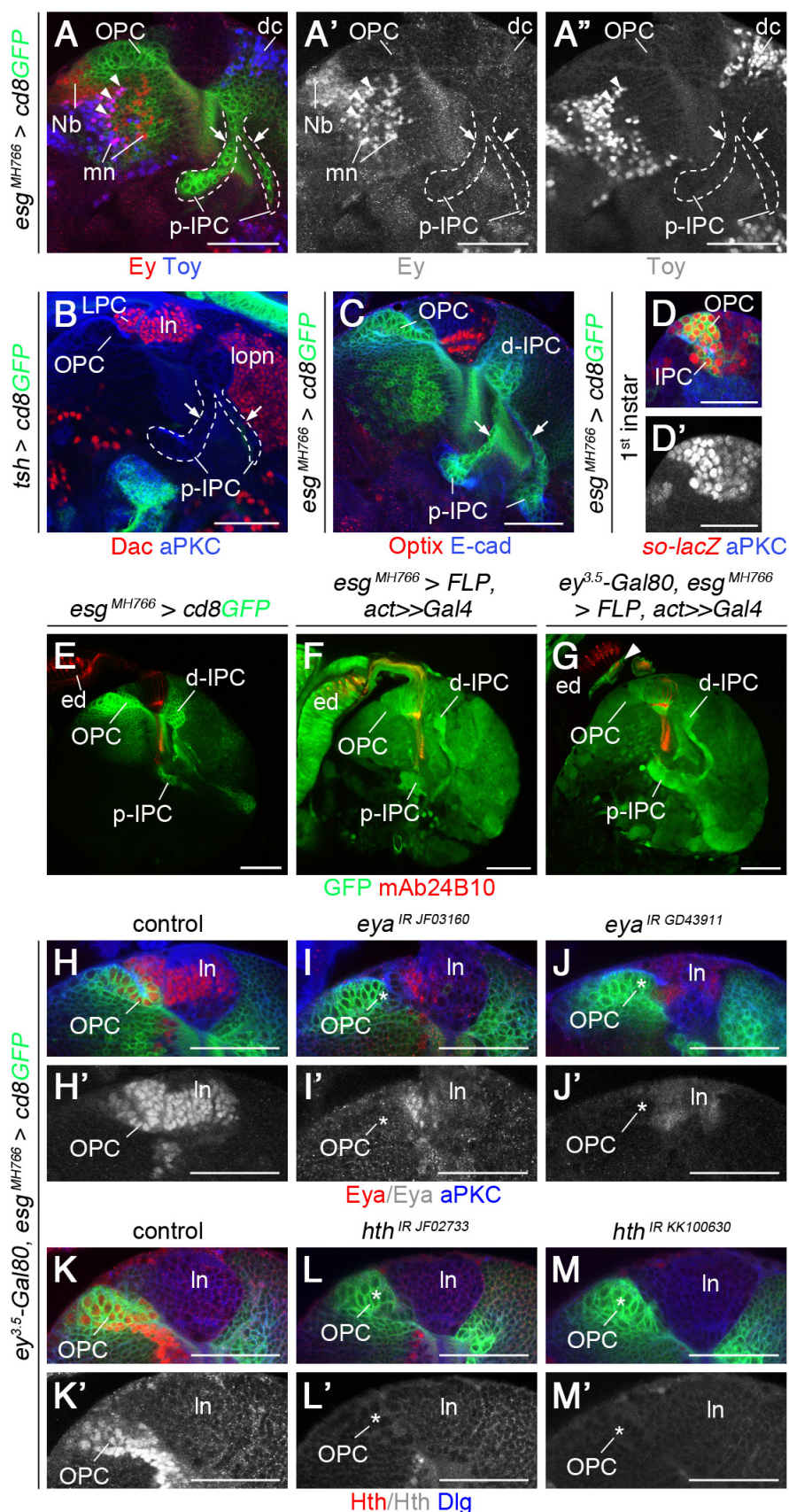


Fig. S3. Expression of RDGN members in the OPC and IPC and validation of tools for RNAi-mediated knockdown in the OPC. Optic lobes were labeled with *esg^{MH766}-Gal4*, *UAS-cd8GFP* (green; A,C,D) and *E-cad* (blue; C). (A-A'') At the third instar larval stage, *Ey* (red; white in A') and

Toy (blue; white in A'') were not expressed in OPC or p-IPC NE cells and cell streams (outlined; arrows indicate cell streams). Ey was expressed in a subset of OPC Nbs and two domains of medulla neurons (mn). One domain co-expressed Toy (arrowheads). Toy was expressed in a subpopulation of distal cells (dc). (B) Dac (red) was expressed in lamina precursor cells (LPC), differentiating lamina neurons (ln) and lobula plate neurons (lopn), but not in OPC or p-IPC NE cells. *tsh-Gal4 UAS-cd8GFP* (green) was not detected in the optic lobe, co-labeled with aPKC (blue). (C) Optix (red) is not expressed in the p-IPC and cell streams. Optix was detected in dorso-ventral OPC subdomains (cf. Fig. 7F), not in plane in this horizontal view of the central OPC domain. Epithelial and marginal lamina glial cells were labeled by Optix. (D,D') In first instar larval optic lobes labeled with aPKC (blue), *so-lacZ* (red) was expressed in the OPC and IPC. (E-G) At the third instar larval stage, *esg^{MH766}-Gal4, UAS-cd8GFP* (green; E) was specifically expressed in the optic lobe, and not the eye disc (ed). Monitoring *esg^{MH766}-Gal4* activity during early larval development using the *FLPout* approach revealed GFP expression (green; F) in the eye disc. *ey^{3.5}-Gal80* suppressed *esg^{MH766}-Gal4* activity in eye discs during development (G). GFP expression was detected in glial cells (arrowhead) that originated from the optic stalk, but not in R-cells labeled with mAb24B10 (red). (H-M) In controls, Eya (red, H) and Hth (red, K) were expressed in NE cells of the OPC. In addition, Eya was detected in lamina neurons (ln), and Hth in a subset of OPC Nbs and medulla neurons. Expression of two different RNAi transgenes for *eya* and *hth - eya^{IR JF03160}* (I,I'), *eya^{IR GD43911}* (J,J'), *hth^{IR JF02733}* (L,L'), and *hth^{IR KK100630}* (M,M') – using *esg^{MH766}-Gal4* resulted in efficient knockdown of Eya and Hth expression in OPC NE cells (red, asterisks). For genotypes and sample numbers, see **Table S2**. Related to **Fig. 5**. Scale bars: 50 µm (A-C, E-M), 25 µm (D).

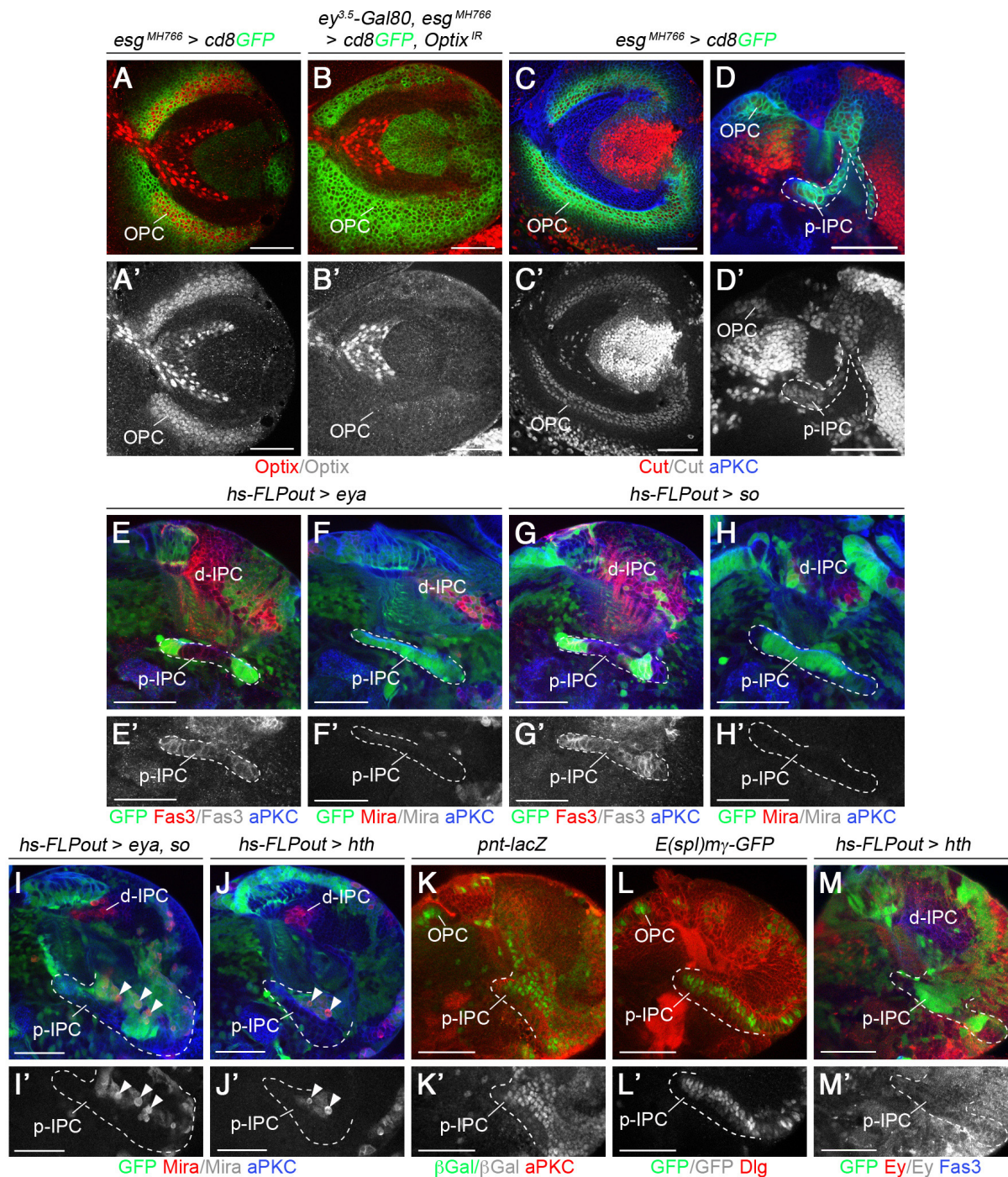


Fig. S4. Validation of Optix RNAi-mediated knockdown, assessment of Cut, pnt-lacZ and E(spl)m γ -GFP expression in the optic lobe and effects of ectopic expression of eya, so, and hth in the p-IPC. (A-B') Compared to controls (A,A'), expression of an Optix RNAi transgene – Optix^{IR}_{JF02199} – using esg^{MH766}-Gal4 (B,B') resulted in efficient knockdown of Optix (red) in dorso-ventral OPC subdomains. Optix expression in glial cells is not affected. (C-D') Optic lobes labeled with esg^{MH766}-Gal4, UAS-cd8GFP (green) and aPKC (blue) are shown in lateral (C,C') and horizontal views (D,D'). Cut (red) was expressed in OPC and p-IPC NE cells and cell streams (D; outlined). Cut expression was increased in the oldest neuronal progeny of the OPC and IPC. (E-H') In hs-FLPout clones (green) expressing eya (E-F') or so (G-H') in the p-IPC Fas3 was not downregulated (red; E,G), and the formation of Mira-positive Nbs was not induced (red; F,H). (I-J') Ectopic eya/so (I,I') and hth (J,J') induced the formation of Mira-positive Nbs (red) in the p-IPC. (K-L') pnt-lacZ (green;

K,K') and *E(spl)mγ-GFP* (green; L) were expressed in the OPC and p-IPC (dotted line). (M,M') Ectopic *hth* did not promote the formation of Ey positive Nbs (red) in the p-IPC. Related to **Figs. 7,8**. For genotypes and sample numbers, see **Table S2**. Scale bars: 50 μm.

Table S1. Full genotypes and sample numbers shown in main figure panels.

Figure	Panel	Genotype	n= ^a
Fig. 1	C	<i>ey</i> ^{3.5} - <i>Gal80/w</i> ¹¹¹⁸ or <i>Y</i> ; <i>esg</i> ^{MH766} - <i>Gal4</i> /+; <i>UAS-Dcr2 UAS-cd8GFP/+</i>	9
	D'	<i>ey</i> ^{3.5} - <i>Gal80</i> /+ or <i>Y</i> ; <i>FRT42D ubi-GFP PCNA</i> ⁷⁷⁵ / <i>FRT42D</i> ; <i>lama-Gal4</i> <i>UAS-FLP mδ/ro-τ-lacZ</i>	8
	D''	<i>ey</i> ^{3.5} - <i>Gal80</i> /+ or <i>Y</i> ; <i>FRT42D ubi-GFP PCNA</i> ⁷⁷⁵ / <i>FRT42D</i> 3-78; <i>lama-</i> <i>Gal4 UAS-FLP mδ/ro-τ-lacZ</i>	14
	E	<i>ey</i> ^{3.5} - <i>Gal80</i> /+ or <i>Y</i> ; <i>FRT42D ubi-GFP PCNA</i> ⁷⁷⁵ / <i>FRT42D</i> ; <i>lama-Gal4</i> <i>UAS-FLP mδ/+</i>	31
	F	<i>ey</i> ^{3.5} - <i>Gal80</i> /+ or <i>Y</i> ; <i>FRT42D ubi-GFP PCNA</i> ⁷⁷⁵ / <i>FRT42D</i> ; <i>lama-Gal4</i> <i>UAS-FLP mδ/+</i>	4
	G	<i>ey</i> ^{3.5} - <i>Gal80</i> /+ or <i>Y</i> ; <i>FRT42D ubi-GFP PCNA</i> ⁷⁷⁵ / <i>FRT42D</i> 3-78; <i>lama-</i> <i>Gal4 UAS-FLP mδ/+</i>	40
	H	<i>ey</i> ^{3.5} - <i>Gal80</i> /+ or <i>Y</i> ; <i>FRT42D ubi-GFP PCNA</i> ⁷⁷⁵ / <i>FRT42D</i> 3-78; <i>lama-</i> <i>Gal4 UAS-FLP mδ/+</i>	7
	J,K	<i>ey</i> ^{3.5} - <i>Gal80</i> /+ or <i>Y</i> ; <i>FRT42D ubi-GFP PCNA</i> ⁷⁷⁵ / <i>FRT42D Pcl</i> ^{3-78*38} ; <i>lama-</i> <i>Gal4 UAS-FLP mδ/+</i>	107 ^b , 60 ^c , 22 ^d
	M	<i>ey</i> ^{3.5} - <i>Gal80</i> /+ or <i>Y</i> ; <i>FRT42D ubi-GFP PCNA</i> ⁷⁷⁵ / <i>FRT42D</i> ; <i>lama-Gal4</i> <i>UAS-FLP mδ/h-lacZ</i> ⁰⁸²⁴⁷	11
	N	<i>ey</i> ^{3.5} - <i>Gal80</i> /+ or <i>Y</i> ; <i>FRT42D ubi-GFP PCNA</i> ⁷⁷⁵ / <i>FRT42D Pcl</i> ^{3-78*38} ; <i>lama-</i> <i>Gal4 UAS-FLP mδ/h-lacZ</i> ⁰⁸²⁴⁷	8
Fig. 2	A	<i>ey</i> ^{3.5} - <i>Gal80</i> /+ or <i>Y</i> ; <i>FRT42D ubi-GFP PCNA</i> ⁷⁷⁵ / <i>FRT42D</i> ; <i>lama-Gal4</i> <i>UAS-FLP mδ/+</i>	31
	B,C	<i>ey</i> ^{3.5} - <i>Gal80</i> /+ or <i>Y</i> ; <i>FRT42D ubi-GFP PCNA</i> ⁷⁷⁵ / <i>FRT42D Pcl</i> ^{3-78*38} ; <i>lama-</i> <i>Gal4 UAS-FLP mδ/+</i>	107
	D	<i>ey</i> ^{3.5} - <i>Gal80</i> /+ or <i>Y</i> ; <i>FRT42D ubi-GFP PCNA</i> ⁷⁷⁵ / <i>FRT42D Pcl</i> ^{3-78*38} ; <i>lama-</i> <i>Gal4 UAS-FLP mδ/dpp-lacZ</i> ^{Exel.2}	10/11
	E	<i>y w ey-FLP/+</i> or <i>Y</i> ; <i>FRT42D ubi-GFP PCNA</i> ⁷⁷⁵ / <i>FRT42D</i> ; <i>h-lacZ</i> ⁰⁸²⁴⁷ /+	8
	F	<i>y w ey-FLP/+</i> or <i>Y</i> ; <i>FRT42D ubi-GFP PCNA</i> ⁷⁷⁵ / <i>FRT42D Pcl</i> ^{3-78*38} ; <i>h-</i> <i>lacZ</i> ⁰⁸²⁴⁷ /+	6
	G	<i>ey</i> ^{3.5} - <i>Gal80</i> /+ or <i>Y</i> ; <i>FRT42D ubi-GFP PCNA</i> ⁷⁷⁵ / <i>FRT42D Pcl</i> ^{3-78*38} ; <i>lama-</i> <i>Gal4 UAS-FLP mδ/+</i>	7/10
	H	<i>ey</i> ^{3.5} - <i>Gal80</i> /+ or <i>Y</i> ; <i>FRT42D ubi-GFP PCNA</i> ⁷⁷⁵ / <i>FRT42D Pcl</i> ^{3-78*38} ; <i>lama-</i> <i>Gal4 UAS-FLP mδ/+</i>	7
	I	<i>ey</i> ^{3.5} - <i>Gal80</i> /+ or <i>Y</i> ; <i>FRT42D ubi-GFP PCNA</i> ⁷⁷⁵ / <i>FRT42D Pcl</i> ^{3-78*38} ; <i>lama-</i> <i>Gal4 UAS-FLP mδ/+</i>	17
	J	<i>neur</i> ^{P72} - <i>Gal4 UAS-pon-GFP/UAS-cd8GFP</i>	6
	L	<i>ey</i> ^{3.5} - <i>Gal80</i> /+ or <i>Y</i> ; <i>FRT42D ubi-GFP PCNA</i> ⁷⁷⁵ / <i>FRT42D Pcl</i> ^{3-78*38} ; <i>lama-</i> <i>Gal4 UAS-FLP mδ/+</i>	11
	M	<i>ey</i> ^{3.5} - <i>Gal80</i> /+ or <i>Y</i> ; <i>FRT42D ubi-GFP PCNA</i> ⁷⁷⁵ / <i>FRT42D Pcl</i> ^{3-78*38} ; <i>lama-</i> <i>Gal4 UAS-FLP mδ/+</i>	8
	N	<i>w hs-FLP</i> ¹²² <i>elav-Gal4</i> ^{c155} <i>UAS-cd8GFP/+</i> or <i>Y</i> ; <i>FRT42D tubP-</i> <i>Gal80/FRT42D Pcl</i> ^{3-78*38} ; <i>tubP-Gal4/+</i>	40 ^e
	O	<i>elav-Gal4</i> ^{c155} <i>hs-FLP</i> ¹ /+ or <i>Y</i> ; <i>tubP-Gal4/UAS-cd8GFP</i> ; <i>FRT82B tubP-</i> <i>Gal80/FRT82B Sce</i> ¹	14 ^f
Fig. 3	A	<i>ey</i> ^{3.5} - <i>Gal80</i> /+ or <i>Y</i> ; <i>FRT42D ubi-GFP PCNA</i> ⁷⁷⁵ / <i>FRT42D</i> ; <i>lama-Gal4</i> <i>UAS-FLP mδ/+</i>	3
	B,C	<i>ey</i> ^{3.5} - <i>Gal80</i> /+ or <i>Y</i> ; <i>FRT42D ubi-GFP PCNA</i> ⁷⁷⁵ / <i>FRT42D Pcl</i> ^{3-78*38} ; <i>lama-</i> <i>Gal4 UAS-FLP mδ/+</i>	16
	D	<i>ey</i> ^{3.5} - <i>Gal80</i> /+ or <i>Y</i> ; <i>FRT42D ubi-GFP PCNA</i> ⁷⁷⁵ / <i>FRT42D</i> ; <i>lama-Gal4</i> <i>UAS-FLP mδ/+</i>	2
	E	<i>ey</i> ^{3.5} - <i>Gal80</i> /+ or <i>Y</i> ; <i>FRT42D ubi-GFP PCNA</i> ⁷⁷⁵ / <i>FRT42D Pcl</i> ^{3-78*38} ; <i>lama-</i> <i>Gal4 UAS-FLP mδ/+</i>	5
	F	<i>ey</i> ^{3.5} - <i>Gal80</i> /+ or <i>Y</i> ; <i>FRT42D ubi-GFP PCNA</i> ⁷⁷⁵ / <i>FRT42D</i> ; <i>lama-Gal4</i> <i>UAS-FLP mδ/+</i>	3
	G	<i>ey</i> ^{3.5} - <i>Gal80</i> /+ or <i>Y</i> ; <i>FRT42D ubi-GFP PCNA</i> ⁷⁷⁵ / <i>FRT42D Pcl</i> ^{3-78*38} ; <i>lama-</i> <i>Gal4 UAS-FLP mδ/+</i>	5

	H	<i>ey</i> ^{3.5} - <i>Gal80</i> /+ or Y; FRT42D <i>ubi-GFP PCNA</i> ⁷⁷⁵ /FRT42D; <i>lama-Gal4 UAS-FLP mδ/+</i>	31
	I	<i>ey</i> ^{3.5} - <i>Gal80</i> /+ or Y; FRT42D <i>ubi-GFP PCNA</i> ⁷⁷⁵ /FRT42D <i>Pcl</i> ^{3-78*38} ; <i>lama-Gal4 UAS-FLP mδ/+</i>	107
	J	<i>ey</i> ^{3.5} - <i>Gal80</i> /+ or Y; FRT42D <i>ubi-GFP PCNA</i> ⁷⁷⁵ /FRT42D <i>Pcl</i> ^{3-78*38} ; <i>lama-Gal4 UAS-FLP mδ/UAS-AbdB</i> ^{IR GD12024}	8
	K	<i>ey</i> ^{3.5} - <i>Gal80</i> /+ or Y; FRT42D <i>ubi-GFP PCNA</i> ⁷⁷⁵ /FRT42D <i>Pcl</i> ^{3-78*38} ; <i>lama-Gal4 UAS-FLP mδ/UAS-AbdB</i> ^{IR GD12024}	18
	L,M	<i>y hs-FLP</i> ¹²² ; <i>act>y+>Gal4 UAS-GFP dpp-lacZ/UAS-AbdB</i>	18
Fig. 4	A	<i>ey</i> ^{3.5} - <i>Gal80</i> /+ or Y; FRT42D <i>ubi-GFP PCNA</i> ⁷⁷⁵ /FRT42D; <i>lama-Gal4 UAS-FLP mδ/dpp-lacZ</i> ^{Exel.2}	5
	B	<i>ey</i> ^{3.5} - <i>Gal80</i> /+ or Y; FRT42D <i>ubi-GFP PCNA</i> ⁷⁷⁵ /FRT42D <i>Pcl</i> ^{3-78*38} ; <i>lama-Gal4 UAS-FLP mδ/dpp-lacZ</i> ^{Exel.2}	15
	C	<i>ey</i> ^{3.5} - <i>Gal80</i> /+ or Y; FRT42D <i>ubi-GFP PCNA</i> ⁷⁷⁵ /FRT42D; <i>lama-Gal4 UAS-FLP mδ/+</i>	31
	D	<i>ey</i> ^{3.5} - <i>Gal80</i> /+ or Y; FRT42D <i>ubi-GFP PCNA</i> ⁷⁷⁵ /FRT42D <i>Pcl</i> ^{3-78*38} ; <i>lama-Gal4 UAS-FLP mδ/dpp-lacZ</i> ^{Exel.2}	9/10
	E	<i>ey</i> ^{3.5} - <i>Gal80</i> /+ or Y; FRT42D <i>ubi-GFP PCNA</i> ⁷⁷⁵ /FRT42D <i>Pcl</i> ^{3-78*38} ; <i>lama-Gal4 UAS-FLP mδ/+</i>	5
	F	<i>y hs-FLP</i> ¹²² ; <i>act>y+>Gal4 UAS-GFP dpp-lacZ/UAS-AbdB</i>	10
	H	<i>esg</i> ^{MH766} - <i>Gal4/CyO</i> or <i>Pin</i> ^{YT} ; <i>UAS-cd8GFP/UAS-cd8GFP</i>	11
	I	<i>w hs-FLP</i> ¹²² <i>elav-Gal4</i> ¹⁵⁵ <i>UAS-cd8GFP/+</i> or Y; FRT42D <i>tubP-Gal80/FRT42D Pcl</i> ^{3-78*38} ; <i>tubP-Gal4/+</i>	5/8
	J	<i>y hs-FLP</i> ¹²² ; <i>act>y+>Gal4 UAS-GFP dpp-lacZ/UAS-AbdB</i>	14 ^g
Fig. 5	A	<i>esg</i> ^{MH766} - <i>Gal4/CyO</i> or <i>Pin</i> ^{YT} ; <i>UAS-cd8GFP/UAS-cd8GFP</i>	11
	B	<i>esg</i> ^{MH766} - <i>Gal4/so⁷-lacZ</i> ; <i>UAS-cd8GFP/+</i>	3
	C	<i>esg</i> ^{MH766} - <i>Gal4/CyO</i> or <i>Pin</i> ^{YT} ; <i>UAS-cd8GFP/UAS-cd8GFP</i>	3
	D	<i>esg</i> ^{MH766} - <i>Gal4/so⁷-lacZ</i> ; <i>UAS-cd8GFP/UAS-cd8GFP</i>	10
	E	<i>esg</i> ^{MH766} - <i>Gal4/CyO</i> or <i>Pin</i> ^{YT} ; <i>UAS-cd8GFP/UAS-cd8GFP</i>	6
	G	<i>ey</i> ^{3.5} - <i>Gal80</i> /+ or Y; <i>esg</i> ^{MH766} - <i>Gal4/so⁷-lacZ</i> ; <i>UAS-Dcr2 UAS-cd8GFP/UAS-eya</i> ^{IR TRIP.JF03160}	8
	H	<i>ey</i> ^{3.5} - <i>Gal80</i> /+ or Y; <i>ubi-GFP cycE</i> ^{AR95} FRT40A/ <i>eya</i> ^{clifl} FRT40A; <i>lama-Gal4 UAS-FLP mδ/+</i>	11
	I	<i>ey</i> ^{3.5} - <i>Gal80</i> /+ or Y; FRT42D <i>ubi-GFP PCNA</i> ⁷⁷⁵ /FRT42D <i>so³</i> ; <i>lama-Gal4 UAS-FLP mδ/+</i>	14
	J	<i>ey</i> ^{3.5} - <i>Gal80</i> /+ or Y; FRT42D <i>ubi-GFP PCNA</i> ⁷⁷⁵ /FRT42D <i>so³</i> ; <i>lama-Gal4 UAS-FLP mδ/+</i>	12
	K	<i>ey</i> ^{3.5} - <i>Gal80</i> /+ or Y; <i>esg</i> ^{MH766} - <i>Gal4/UAS-so</i> ^{IR KK104386} ; <i>UAS-Dcr2 UAS-cd8GFP/UAS-eya</i> ^{IR TRIP.JF03160}	6
	L	<i>ey</i> ^{3.5} - <i>Gal80</i> /+ or Y; <i>esg</i> ^{MH766} - <i>Gal4/+</i> ; <i>UAS-Dcr2 UAS-cd8GFP/UAS-hth</i> ^{IR TRIP.JF02733}	5
	M	<i>ey</i> ^{3.5} - <i>Gal80</i> /+ or Y; <i>esg</i> ^{MH766} - <i>Gal4/so⁷-lacZ</i> ; <i>UAS-Dcr2 UAS-cd8GFP/UAS-hth</i> ^{IR TRIP.JF02733}	7
	N	<i>ey</i> ^{3.5} - <i>Gal80</i> /+ or Y; <i>esg</i> ^{MH766} - <i>Gal4/UAS-so</i> ^{IR KK104386} ; <i>UAS-Dcr2 UAS-cd8GFP/UAS-hth</i> ^{IR TRIP.JF02733}	5
Fig. 6	B	<i>ey</i> ^{3.5} - <i>Gal80/w</i> ¹¹¹⁸ or Y; <i>esg</i> ^{MH766} - <i>Gal4/+</i> ; <i>UAS-Dcr2 UAS-cd8GFP/+</i>	4
	C	<i>ey</i> ^{3.5} - <i>Gal80</i> /+ or Y; <i>esg</i> ^{MH766} - <i>Gal4/UAS-so</i> ^{IR KK104386} ; <i>UAS-Dcr2 UAS-cd8GFP/UAS-eya</i> ^{IR TRIP.JF03160}	10/11 ^h
	D	<i>ey</i> ^{3.5} - <i>Gal80</i> /+ or Y; <i>esg</i> ^{MH766} - <i>Gal4/UAS-so</i> ^{IR KK104386} ; <i>UAS-Dcr2 UAS-cd8GFP/UAS-eya</i> ^{IR TRIP.JF03160}	10/11 ⁱ
	E	<i>ey</i> ^{3.5} - <i>Gal80</i> /+ or Y; <i>esg</i> ^{MH766} - <i>Gal4/UAS-so</i> ^{IR KK104386} ; <i>UAS-Dcr2 UAS-cd8GFP/UAS-eya</i> ^{IR TRIP.JF03160}	5/11 ^j
	G	<i>ey</i> ^{3.5} - <i>Gal80/w</i> ¹¹¹⁸ or Y; <i>esg</i> ^{MH766} - <i>Gal4/+</i> ; <i>UAS-Dcr2 UAS-cd8GFP/+</i>	7
	H	<i>ey</i> ^{3.5} - <i>Gal80</i> /+ or Y; <i>esg</i> ^{MH766} - <i>Gal4/UAS-so</i> ^{IR KK104386} ; <i>UAS-Dcr2 UAS-cd8GFP/UAS-eya</i> ^{IR TRIP.JF03160}	9/12 ^k
	I	<i>ey</i> ^{3.5} - <i>Gal80/w</i> ¹¹¹⁸ or Y; <i>esg</i> ^{MH766} - <i>Gal4/+</i> ; <i>UAS-Dcr2 UAS-cd8GFP/+</i>	8
	J	<i>ey</i> ^{3.5} - <i>Gal80</i> /+ or Y; <i>esg</i> ^{MH766} - <i>Gal4/UAS-so</i> ^{IR KK104386} ; <i>UAS-Dcr2 UAS-cd8GFP/UAS-eya</i> ^{IR TRIP.JF03160}	10
	K	<i>ey</i> ^{3.5} - <i>Gal80/w</i> ¹¹¹⁸ or Y; <i>esg</i> ^{MH766} - <i>Gal4/+</i> ; <i>UAS-Dcr2 UAS-cd8GFP/+</i>	4

L	<i>ey</i> ^{3.5} - <i>Gal80</i> /+ or Y; <i>esg</i> ^{MH766} - <i>Gal4/UAS-so</i> ^{IR KK104386} ; <i>UAS-Dcr2 UAS-cd8GFP/UAS-eya</i> ^{IR TRIP.JF03160}	8
M	<i>ey</i> ^{3.5} - <i>Gal80</i> /+ or Y; <i>esg</i> ^{MH766} - <i>Gal4</i> /+; <i>UAS-Dcr2 UAS-cd8GFP/UAS-hth</i> ^{IR TRIP.JF02733}	6
N	<i>ey</i> ^{3.5} - <i>Gal80/w</i> ¹¹¹⁸ or Y; <i>esg</i> ^{MH766} - <i>Gal4</i> /+; <i>UAS-Dcr2 UAS-cd8GFP/+</i>	9
O	<i>ey</i> ^{3.5} - <i>Gal80</i> /+ or Y; <i>esg</i> ^{MH766} - <i>Gal4</i> /+; <i>UAS-Dcr2 UAS-cd8GFP/UAS-hth</i> ^{IR TRIP.JF02733}	9
Q	<i>ey</i> ^{3.5} - <i>Gal80/w</i> ¹¹¹⁸ or Y; <i>esg</i> ^{MH766} - <i>Gal4</i> /+; <i>UAS-Dcr2 UAS-cd8GFP/+</i>	5
R	<i>ey</i> ^{3.5} - <i>Gal80</i> /+ or Y; <i>esg</i> ^{MH766} - <i>Gal4</i> /+; <i>UAS-Dcr2 UAS-cd8GFP/UAS-hth</i> ^{IR TRIP.JF02733}	10
Fig. 7	A <i>ey</i> ^{3.5} - <i>Gal80</i> /+ or Y; <i>ubi-GFP cycE</i> ^{AR95} <i>FRT40A/eya</i> ^{clif1} <i>FRT40A; lama-Gal4 UAS-FLP mδ/+</i>	5
	B <i>ey</i> ^{3.5} - <i>Gal80</i> /+ or Y; <i>FRT42D ubi-GFP PCNA</i> ⁷⁷⁵ / <i>FRT42D so</i> ³ ; <i>lama-Gal4 UAS-FLP mδ/+</i>	7
	C <i>ey</i> ^{3.5} - <i>Gal80</i> /+ or Y; <i>ubi-GFP cycE</i> ^{AR95} <i>FRT40A/eya</i> ^{clif1} <i>FRT40A; lama-Gal4 UAS-FLP mδ/+</i>	9
	D <i>elav-Gal4</i> ^{c155} <i>hs-FLP</i> ¹ /+ or Y; <i>tubP-Gal4/UAS-cd8GFP; FRT82B tubP-Gal80/FRT82B hth</i> ^{64.1}	9
	E <i>ey</i> ^{3.5} - <i>Gal80/UAS-eya</i> ^{IR GD43911} ; <i>esg</i> ^{MH766} - <i>Gal4/UAS-so</i> ^{IR KK104386} ; <i>UAS-Dcr2 UAS-cd8GFP/UAS-hth</i> ^{IR TRIP.JF02733}	5
	F <i>esg</i> ^{MH766} - <i>Gal4/CyO</i> or <i>Pin</i> ^Y ; <i>UAS-cd8GFP/UAS-cd8GFP</i>	7
	G <i>ey</i> ^{3.5} - <i>Gal80/UAS-eya</i> ^{IR GD43911} ; <i>esg</i> ^{MH766} - <i>Gal4/UAS-hth</i> ^{IR KK100630} ; <i>UAS-Dcr2 UAS-cd8GFP/UAS-Optix</i> ^{IR TRIP.JF02199}	8
	H,I <i>ey</i> ^{3.5} - <i>Gal80</i> /+ or Y; <i>FRT42D ubi-GFP PCNA</i> ⁷⁷⁵ / <i>FRT42D Pcl</i> ^{3-78*38} ; <i>lama-Gal4 UAS-FLP mδ/+</i>	11/12 ^l , 13/13 ^m
	J,K <i>ey</i> ^{3.5} - <i>Gal80</i> /+ or Y; <i>FRT42D ubi-GFP PCNA</i> ⁷⁷⁵ / <i>FRT42D Pcl</i> ^{3-78*38} ; <i>lama-Gal4 UAS-FLP mδ/+</i>	10/11 ⁿ , 12/12 ^o
	L <i>y hs-FLP</i> ¹²² ; <i>act>y>Gal4 UAS-GFP dpp-lacZ/UAS-AbdB</i>	6
	M <i>y hs-FLP</i> ¹²² ; <i>act>y>Gal4 UAS-GFP dpp-lacZ/UAS-AbdB</i>	18
	N <i>y hs-FLP</i> ¹²² ; <i>act>y>Gal4 UAS-GFP dpp-lacZ/UAS-AbdB</i>	6
	O <i>y hs-FLP</i> ¹²² ; <i>act>y>Gal4 UAS-GFP dpp-lacZ/UAS-AbdB</i>	13
Fig. 8	A <i>y hs-FLP</i> ¹²² ; <i>act>y>Gal4 UAS-GFP dpp-lacZ/+; UAS-so UAS-eya/+</i>	7
	B <i>y hs-FLP</i> ¹²² ; <i>act>y>Gal4 UAS-GFP dpp-lacZ/+; UAS-so UAS-eya/+</i>	12
	C <i>y hs-FLP</i> ¹²² ; <i>act>y>Gal4 UAS-GFP dpp-lacZ/+; UAS-hth</i> ¹² /+	11
	D <i>y hs-FLP</i> ¹²² ; <i>act>y>Gal4 UAS-GFP dpp-lacZ/+; UAS-hth</i> ¹² /+	18
	E <i>y hs-FLP</i> ¹²² ; <i>act>y>Gal4 UAS-GFP dpp-lacZ/+; UAS-so UAS-eya/+</i>	6
	F <i>y hs-FLP</i> ¹²² ; <i>act>y>Gal4 UAS-GFP dpp-lacZ/+; UAS-so UAS-eya/+</i>	13
	G <i>y hs-FLP</i> ¹²² ; <i>act>y>Gal4 UAS-GFP dpp-lacZ/+; UAS-so UAS-eya/+</i>	7
	H <i>y hs-FLP</i> ¹²² ; <i>act>y>Gal4 UAS-GFP dpp-lacZ/+; TM3/+</i>	4
	I <i>y hs-FLP</i> ¹²² ; <i>act>y>Gal4 UAS-GFP dpp-lacZ/+; UAS-so UAS-eya/+</i>	13
	J <i>y hs-FLP</i> ¹²² ; <i>act>y>Gal4 UAS-GFP dpp-lacZ/+; TM3/+</i>	2
	K <i>y hs-FLP</i> ¹²² ; <i>act>y>Gal4 UAS-GFP dpp-lacZ/+; UAS-so UAS-eya/+</i>	5

> indicate FRT sites;

^a If not otherwise indicated, in loss-of-function and knockdown experiments, all examined control samples were normal, while all experimental samples showed defects (100% penetrance);^b large Fas3-positive NE cell clusters; ^c small OPC NE cell clusters; ^d small IPC NE cell clusters;^e 41/47 clones in the OPC showed ectopic Fas3; ^f 21/21 clones in the OPC showed ectopic Fas3;^g 32/69 Abd-B positive progenitor cells expressed Ase;^h show N^{ICD} localization defects; ⁱ show ectopic Nbs/GMCs; ^j have areas with Nbs only; ^k show L'sc labeling in more than 4 cells;^l Eya levels reduced in small OPC clusters; ^m Eya levels reduced in large OPC clusters;ⁿ Hth levels reduced in small OPC clusters; ^o Hth levels reduced in large OPC clusters.

Table S2. Full genotypes and sample numbers shown in Supplementary figure panels.

Figure	Panel	Genotype	n= ^a
Fig. S1	B	<i>ey</i> ^{3.5} - <i>Gal80</i> /+ or <i>Y</i> ; <i>FRT42D ubi-GFP PCNA</i> ⁷⁷⁵ / <i>FRT42D 3-78*56</i> ; <i>lama-Gal4 UAS-FLP mδ/+</i>	16
	C	<i>ey</i> ^{3.5} - <i>Gal80</i> /+ or <i>Y</i> ; <i>FRT42D ubi-GFP PCNA</i> ⁷⁷⁵ / <i>FRT42D Pcl</i> ^{3-78*38} ; <i>lama-Gal4 UAS-FLP mδ/+</i>	107
	D	<i>ey</i> ^{3.5} - <i>Gal80</i> /+ or <i>Y</i> ; <i>FRT42D ubi-GFP PCNA</i> ⁷⁷⁵ / <i>FRT42D Pcl</i> ^{3-78*38} ; <i>lama-Gal4 UAS-FLP mδ/ro-τ-lacZ</i>	8
	E	<i>ey</i> ^{3.5} - <i>Gal80</i> /+ or <i>Y</i> ; <i>FRT42D ubi-GFP PCNA</i> ⁷⁷⁵ / <i>FRT40A FRT42D y⁺ Pcl</i> ^{777a} ; <i>lama-Gal4 UAS-FLP mδ/+</i>	28
	F	<i>ey</i> ^{3.5} - <i>Gal80</i> /+ or <i>Y</i> ; <i>FRT42D ubi-GFP PCNA</i> ⁷⁷⁵ / <i>FRT40A FRT42D y⁺ Pcl</i> ^{777a} ; <i>lama-Gal4 UAS-FLP mδ/+</i>	7
	G	<i>neur</i> ^{P72} - <i>Gal4 UAS-pon-GFP/UAS-cd8GFP</i>	9
Fig. S2	A	<i>ey</i> ^{3.5} - <i>Gal80</i> /+ or <i>Y</i> ; <i>FRT42D ubi-GFP PCNA</i> ⁷⁷⁵ / <i>FRT42D; lama-Gal4 UAS-FLP mδ/+</i>	6
	B	<i>ey</i> ^{3.5} - <i>Gal80</i> /+ or <i>Y</i> ; <i>FRT42D ubi-GFP PCNA</i> ⁷⁷⁵ / <i>FRT42D Pcl</i> ^{3-78*38} ; <i>lama-Gal4 UAS-FLP mδ/+</i>	3
	C	<i>ey</i> ^{3.5} - <i>Gal80</i> /+ or <i>Y</i> ; <i>FRT42D ubi-GFP PCNA</i> ⁷⁷⁵ / <i>FRT42D; lama-Gal4 UAS-FLP mδ/+</i>	6
	D	<i>ey</i> ^{3.5} - <i>Gal80</i> /+ or <i>Y</i> ; <i>FRT42D ubi-GFP PCNA</i> ⁷⁷⁵ / <i>FRT42D Pcl</i> ^{3-78*38} ; <i>lama-Gal4 UAS-FLP mδ/+</i>	5
	E	<i>ey</i> ^{3.5} - <i>Gal80</i> /+ or <i>Y</i> ; <i>FRT42D ubi-GFP PCNA</i> ⁷⁷⁵ / <i>FRT42D; lama-Gal4 UAS-FLP mδ/+</i>	6
	F	<i>ey</i> ^{3.5} - <i>Gal80</i> /+ or <i>Y</i> ; <i>FRT42D ubi-GFP PCNA</i> ⁷⁷⁵ / <i>FRT42D Pcl</i> ^{3-78*38} ; <i>lama-Gal4 UAS-FLP mδ/+</i>	5
Fig. S3	A	<i>esg</i> ^{MH766} - <i>Gal4/CyO</i> or <i>Pin</i> ^{YT} ; <i>UAS-cd8GFP/UAS-cd8GFP</i>	3
	B	<i>tsh</i> ^{md621} - <i>Gal4/CyO</i> or <i>Pin</i> ^{YT} ; <i>UAS-cd8GFP/+</i>	7
	C	<i>esg</i> ^{MH766} - <i>Gal4/CyO</i> or <i>Pin</i> ^{YT} ; <i>UAS-cd8GFP/UAS-cd8GFP</i>	4
	D	<i>esg</i> ^{MH766} - <i>Gal4/so⁷-lacZ</i> ; <i>UAS-cd8GFP/UAS-cd8GFP</i>	5
	E	<i>esg</i> ^{MH766} - <i>Gal4/CyO</i> or <i>Pin</i> ^{YT} ; <i>UAS-cd8GFP/+</i>	3
	F	<i>esg</i> ^{MH766} - <i>Gal4/act>y⁺>Gal4 UAS-GFP</i> ; <i>UAS-FLP/+</i>	3
	G	<i>ey</i> ^{3.5} - <i>Gal80</i> /+ or <i>Y</i> ; <i>esg</i> ^{MH766} - <i>Gal4/act>y⁺>Gal4 UAS-GFP</i> ; <i>UAS-FLP/+</i>	5
	H	<i>esg</i> ^{MH766} - <i>Gal4/CyO</i> or <i>Pin</i> ^{YT} ; <i>UAS-cd8GFP/UAS-cd8GFP</i>	11
	I	<i>ey</i> ^{3.5} - <i>Gal80</i> /+ or <i>Y</i> ; <i>esg</i> ^{MH766} - <i>Gal4/+; UAS-Dcr2 UAS-cd8GFP/UAS-eya^{IR} TRIP.JF03160</i>	6
	J	<i>ey</i> ^{3.5} - <i>Gal80/UAS-eya^{IR}GD43911</i> ; <i>esg</i> ^{MH766} - <i>Gal4/+; UAS-Dcr2 UAS-cd8GFP/+</i>	6
	K	<i>ey</i> ^{3.5} - <i>Gal80/w¹¹¹⁸</i> or <i>Y</i> ; <i>esg</i> ^{MH766} - <i>Gal4/+; UAS-Dcr2 UAS-cd8GFP/+</i>	7
	L	<i>ey</i> ^{3.5} - <i>Gal80/+ or Y; esg</i> ^{MH766} - <i>Gal4/+; UAS-Dcr2 UAS-cd8GFP/UAS-hth^{IR} TRIP.JF02733</i>	9
	M	<i>ey</i> ^{3.5} - <i>Gal80/+ or Y; esg</i> ^{MH766} - <i>Gal4/UAS-hth^{IR}KK100630</i> ; <i>UAS-Dcr2 UAS-cd8GFP/+</i>	6
Fig. S4	A	<i>esg</i> ^{MH766} - <i>Gal4/CyO</i> or <i>Pin</i> ^{YT} ; <i>UAS-cd8GFP/UAS-cd8GFP</i>	7
	B	<i>ey</i> ^{3.5} - <i>Gal80/+ or Y; esg</i> ^{MH766} - <i>Gal4/+; UAS-Dcr2 UAS-cd8GFP/UAS-Optix^{IR}TRIP.JF02199</i>	3
	C,D	<i>esg</i> ^{MH766} - <i>Gal4/CyO</i> or <i>Pin</i> ^{YT} ; <i>UAS-cd8GFP/UAS-cd8GFP</i>	3
	E	<i>y hs-FLP</i> ¹²² ; <i>act>y⁺>Gal4 UAS-GFP dpp-lacZ/+; UAS-eya/+</i>	9
	F	<i>y hs-FLP</i> ¹²² ; <i>act>y⁺>Gal4 UAS-GFP dpp-lacZ/+; UAS-eya/+</i>	6
	G	<i>y hs-FLP</i> ¹²² ; <i>act>y⁺>Gal4 UAS-GFP dpp-lacZ/+; UAS-so/+</i>	10
	H	<i>y hs-FLP</i> ¹²² ; <i>act>y⁺>Gal4 UAS-GFP dpp-lacZ/+; UAS-so/+</i>	2
	I	<i>y hs-FLP</i> ¹²² ; <i>act>y⁺>Gal4 UAS-GFP dpp-lacZ/+; UAS-so UAS-eya/+</i>	9
	J	<i>y hs-FLP</i> ¹²² ; <i>act>y⁺>Gal4 UAS-GFP dpp-lacZ/+; UAS-hth¹²/+</i>	11

K	<i>P{PZ}pnt</i> ⁰⁷⁸²⁵ - <i>lacZ</i> /+	3
L	<i>E(spl)mγ-GFP/CyO</i>	3
M	<i>y hs-FLP</i> ¹²² ; <i>act>y+>Gal4 UAS-GFP dpp-lacZ/+; UAS-hth</i> ¹² /+	9

> indicate FRT sites.

^a If not otherwise indicated, in loss-of-function and knockdown experiments, all examined control samples were normal, while all experimental samples showed defects (100% penetrance).

Supplementary Materials and Methods

The following stocks/crosses were used in this study:

- (i) Reporter lines - (1) *ro-τ-lacZ* (Garrity et al., 1999), (2) *h-lacZ*⁰⁸²⁴⁷, (3) *so⁷-lacZ* (Cheyette et al., 1994), (4) *dpp-lacZ*^{Exel.2}, (5) *P{PZ}pnt*⁰⁷⁸²⁵-*lacZ* (Samakovlis et al., 1996) and (6) *E(spl)mγ-GFP* (Almeida and Bray, 2005).
- (ii) *Gal4* lines - (1) *esg*^{MH766}-*Gal4* (Apitz and Salecker, 2015), (2) *w; neur*^{P72}-*Gal4, UAS-pon-GFP/TM6B* (Bellaiche et al., 2001), and (3) *tsh*^{md621}-*Gal4* crossed to (4) *Pin*^{YT}/*CyO; UAS-cd8GFP*; (5) *esg*^{MH766}-*Gal4* crossed to *w; act>y+>Gal4 UAS-GFP; UAS-FLP*; (6) *esg*^{MH766}-*Gal; UAS-cd8GFP* crossed to *so⁷-lacZ/CyO; UAS-cd8GFP*.
- (iii) Loss-of-function analysis using the *ey*^{3.5}-*Gal80, lama-Gal4, UAS-FLP* (ELF) system (Bazigou et al., 2007; Chotard et al., 2005) - (1) ELF 2R: *yw ey*^{3.5}-*Gal80; FRT42D ubi-GFP PCNA*⁷⁷⁵/*CyO; lama-Gal4 UAS-FLP mδ* crossed to (2) *yw; FRT42D*, (3) *yw; FRT42D 3-78/Gla Bc*, (4) *yw; FRT42D Pcl*^{3-78*38}/*Gla Bc*, (5) *yw; FRT42D 3-78*56/Gla Bc*, (6) *y w; FRT40A FRT42D y+ Pcl*^{2777a}/*Gla Bc*, (7) *yw; FRT42D; ro-τ-lacZ*, (8) *yw; FRT42D 3-78/Gla Bc; ro-τ-lacZ*, (9) *yw; FRT42D Pcl*^{3-78*38}/*Gla Bc; ro-τ-lacZ*, (10) *yw; FRT42D 3-78*56/Gla Bc; ro-τ-lacZ*, (11) *yw; FRT42D; h-lacZ*⁰⁸²⁴⁷/*TM6B*, (12) *yw; FRT42D Pcl*^{3-78*38}/*Gla Bc; h-lacZ*⁰⁸²⁴⁷/*TM6B*, (13) *yw; FRT42D; dpp-lacZ*^{Exel.2}, (14) *yw; FRT42D Pcl*^{3-78*38}/*Gla Bc; dpp-lacZ*^{Exel.2}, (15) *yw; FRT42D Pcl*^{3-78*38}/*Gla Bc; UAS-Abd-B*^{IR GD12024}, (16) *FRT42D so*³/*Gla Bc*; (17) ELF 2L: *yw ey*^{3.5}-*Gal80; ubi-GFP cycE*^{AR95} *FRT40A/Gla Bc; lama-Gal4 UAS-FLP mδ* crossed to (18) *yw; FRT40A*, (19) *eya*^{cliffl} *FRT40A/Gla Bc* (3-5, this study; 6, from J. Müller, MPI of Biochemistry, Munich (Gaytan de Ayala Alonso et al., 2007); 16, 19, from F. Pignoni, SUNY Upstate Medical University, Syracuse (Pignoni et al., 1997)).
- (iv) Loss-of-function analysis using the *ey-FLP* transgene (Newsome et al., 2000) - (1) *yw ey-FLP; FRT42D ubi-GFP PCNA*⁷⁷⁵/*CyO* crossed to (2) *yw; FRT42D*, (3) *yw; FRT42D Pcl*^{3-78*38}/*Gla Bc*, (4) *yw; FRT42D; h-lacZ*⁰⁸²⁴⁷/*TM6B*, (5) *yw; FRT42D Pcl*^{3-78*38}/*Gla Bc; h-lacZ*⁰⁸²⁴⁷/*TM6B*.
- (v) Loss-of-function analysis using mosaic analysis with a repressible cell marker (MARCM) (Lee and Luo, 1999) - (1) MARCM 2R: *w hs-FLP*¹²² *elav-Gal4*^{c155} *UAS-cd8GFP; FRT42D tubP-Gal80/CyO* crossed to (2) *yw; FRT42D; tubP-Gal4/TM6B*, (3) *yw; FRT42D Pcl*^{3-78*38}/*Gla Bc; tubP-Gal4/TM6B*; (4) MARCM 3R: *elav-Gal4*^{c155} *hs-FLP*¹; *tubP-Gal4/CyO; FRT82B tubP-Gal80/TM6B* (from A. Gould) crossed to (5) *UAS-cd8GFP/Gla Bc; FRT82B*, (6) *UAS-cd8GFP/Gla Bc; FRT82B hth*^{64.1}/*TM6B*, and (7) *UAS-cd8GFP/Gla Bc; FRT82B Sce*¹/*TM6B*. To induce NE cell clones in the OPC, 24-h embryo collections were heat shocked for 35-70 min at 24-48 h AEL in a 37°C water bath. NE clones in the IPC were generated by heat shocks for 40-50 min at 48-72 h AEL.
- (vi) Knockdown experiments using *UAS-RNAi* transgenes - (1) *yw ey*^{3.5}-*Gal80; esg*^{MH766}-*Gal4; UAS-Dcr2 UAS-cd8GFP/TM6B* crossed to (2) *UAS-hth*^{IR TRiP.JF02733}, (3) *UAS-hth*^{IR KK100630}, (4) *UAS-eya*^{IR TRiP.JF03160}, (5) *UAS-eya*^{IR GD43911}, (6) *UAS-so*^{IR KK104386}, (7) *UAS-Optix*^{IR TRiP.JF02199}, (8) *so⁷-lacZ/Gla Bc; UAS-eya*^{IR TRiP.JF03160}, (9) *so⁷-lacZ/Gla Bc; UAS-hth*^{IR TRiP.JF02733/TM6B}, (10) *UAS-so*^{IR KK104386}; *UAS-eya*^{IR TRiP.JF03160}, (11) *UAS-eya*^{IR GD43911}; *UAS-so*^{IR KK104386}; *UAS-hth*^{IR TRiP.JF02733/TM6B}, and (12) *UAS-eya*^{IR GD43911}; *UAS-hth*^{IR KK100630}; *UAS-Optix*^{IR TRiP.JF02199}.

(vii) Gain-of-function experiments using the *hs-FLPout* approach (Ito et al., 1997; Struhl and Basler, 1993) - (1) *y hs-FLP¹²²; act>y⁺>Gal4 UAS-GFP dpp-lacZ/CyO* flies (from A. Baena-Lopez, University of Oxford) crossed to (2) *UAS-Abd-B* (on II), (3) *UAS-eya* (on III), (4) *UAS-so* (on III), (5) *UAS-hth¹²/TM6B* (Pai et al., 1998), and (6) *UAS-so, UAS-eya/TM6B* (Pignoni et al., 1997). Progeny of crosses were heat shocked at 37°C for 30 min at 96 h AEL (2) or for 30 min at 72 h AEL (3-6).

In ELF and *ey-FLP* mosaics, clones lack GFP, while in MARCM mosaics, clones are labeled with GFP; in *hs-FLPout* mosaics, GFP indicates sites of ectopic gene expression. If not otherwise indicated, stocks were obtained from the Bloomington *Drosophila* Stock Center and are described in FlyBase.

Mutagenesis screen and deficiency mapping

The forward genetic ethane methyl sulphonate (EMS) mutagenesis screen was performed using the ELF approach for chromosome 2R. 1065 independent lines with homozygous mutant lethal mutations on *FRT42D* site-containing second chromosomes were screened for R-cell projection defects at the third instar larval stage. This led to the identification of 3-78 in addition to 29 other mutant lines (Fig. 1D; unpublished observations, H.A., I.S.). Deficiency mapping for 3-78 uncovered three lethal mutations on chromosome arm 2R in the regions 43A4-D3 (with *Df(2R)ED1673* and *Df(2R)ED1715*), 50A1-A7 (with *Df(2R)CX1* and *Df(2R)BSC273*), and 55B5-C2 (with *Df(2R)ED3610* and *Df(2R)BSC334*) (Fig. S1A). These were separated by meiotic recombination into 3-78*38, carrying a lethal mutation in 55B5-C2 and 3-78*56, carrying the other two lethal mutations (Fig. 1I). 3-78 and 3-78*38, but not 3-78*56 ELF mosaic animals displayed similar phenotypes with large Fas3-positive ectopic NE cell clusters in the optic lobe (Fig. S1B,C). The cleaned 3-78*38 allele no longer caused R-cell projection defects (Fig. S1D). When testing the three genes included in 55B5-C2, solely alleles of *Pcl* failed to complement 3-78*38. As both 3-78*38 and 3-78*56 ELF mosaics showed largely normal R-cell projection patterns, the defects observed using the 3-78 mutant chromosome might be caused by genetic interactions of the mutant loci.

Immunolabeling and imaging

The following primary antibodies were used for immunolabeling: mouse mAb24B10 (1:75, Developmental Studies Hybridoma Bank [DSHB]), mouse anti-Abd-B (1A2E9, 1:20, DSHB), rabbit anti-Ase (1:5000, from Y.N. Jan, HHMI, San Francisco, (Brand et al., 1993)), rabbit anti-Ato (1:5000, from Y.N. Jan), mouse anti-Cut (2B10, 1:10, DSHB), guinea pig anti-D (1:200, from J.R. Nambu, University of Massachusetts, Amherst/A. Gould, The Francis Crick Institute, London, (Russell et al., 1996)), mouse anti-Dac (mAbdac2-3, 1:50, DSHB), mouse anti-Dlg (4F3, 1:50, DSHB), guinea pig anti-Dpn (1:500, from J. Skeath, Washington University, St. Louis, (Bier et al., 1992)), rat anti-E-cad (DCAD2, 1:2, DSHB), rat anti-Elav (7E8A10, 1:50, DSHB), rabbit anti-Ey (1.8, 1:200, from U. Walldorf, University of Homburg), mouse anti-Eya (10H6, 1:5, DSHB), mouse anti-Fas3 (7G10, 1:5, DSHB; (Patel et al., 1987; Tayler et al., 2004)), mouse and rabbit anti-β-galactosidase (1:300, Promega; 1:12,000, Cappel), rabbit anti-GFP (1:1000, Molecular Probes), rabbit anti-Hth (1:100, from R. Mann, Columbia University, New York, (Noro et al., 2006)), rat anti-L'sc (1:800, from A. Carmena, Instituto de Neurociencias, Alicante), mouse anti-Mira (PLF81, 1:50, (Ohshiro et al., 2000)), mouse anti-N^{ICD} (C17.9C6, 1:50, DSHB), rabbit anti-Optix (1:200, from F. Pignoni, SUNY Upstate Medical University, Syracuse), rabbit anti-PH3 (1:100, Millipore/Upstate), rabbit anti-aPKC ζ (sc-216, 1:100, Santa Cruz Biotechnologies, (Wodarz et al., 2000)), mouse anti-Pros (MR1A, 1:50, DSHB; (Spana and Doe, 1995)), mouse anti-Repo (8D12, 1:20, DSHB), mouse anti-Scr (6H4.1, 1:20, DSHB), rabbit anti-Slp (54, 1:50, J. Reinitz Segmentation Antibodies, (Kosman et al., 1998)), guinea pig anti-Toy (1.170, 1:200, from U. Walldorf), rabbit anti-Tll (812, 1:20, J. Reinitz Segmentation

Antibodies, (Kosman et al., 1998)), mouse anti-Ubx (FP3.38, 1:20, DSHB) and mouse anti-Wg (4D4, 1:50, DSHB). For immunofluorescence labeling, the following secondary antibodies were used: goat anti-guinea pig, anti-mouse, anti-rabbit, and anti-rat F(ab')₂ fragments coupled to FITC, Cy3 or Cy5/Alexa Fluor 647® (1:400; Jackson ImmunoResearch Laboratories).

Quantifications and statistics

Sample sizes were not pre-calculated, but were based on the standard of the field. In groups of control or experimental animals, larvae and adult flies of the correct stage and genotype were chosen randomly and independently from different vials. Data acquisition and analysis used samples with specific genotypes and was not limited in repeatability.

To compare OPC volumes of wild type and *UAS-hth*^{IR} expressing animals, 11 serial 1 μm -serial optical sections were selected for analysis using Amira 5 (Visage Imaging) from optic lobes that had been imaged in a horizontal orientation before and after the OPC center (defined by the position of the mAb24B10 positive larval optic neuropil).

Mitotic indices are provided as the number of PH3-positive cells per $10^3 \mu\text{m}^3$ of wild type OPC NE cells or Fas3-positive *Pcl*^{3-78*38} mutant cell clusters. OPC NE cells were distinguished from adjacent dividing Nbs and lamina precursor cells by the presence of E-cad and the lack of *neur>cd8GFP* and Dac (Figs. 2J; S1G). An average of 0.18 cells (± 0.07 95% confidence interval) per $10^3 \mu\text{m}^3$ of wild type OPC NE cells undergo mitosis during late third instar larval development. While the average size of Fas3-positive mutant epithelial clusters increased from $30.2 \times 10^3 \mu\text{m}^3$ at 114 h AEL ($n=7$) to $52.4 \times 10^3 \mu\text{m}^3$ at the wandering third instar larval stage ($n=13$), the average of mitotic cells at these time points remained constant (0.087 ± 0.04 and 0.09 ± 0.03 95% confidence interval, respectively).

To determine the number of migratory progenitors that differentiate prematurely into Nbs, $y\hspace{0.1em} hs\text{-}FLP^{122}; act>y^+>Gal4\ UAS\text{-}GFP\ dpp\text{-}lacZ/UAS\text{-}Abd\text{-}B$ larvae were heat shocked at 37°C for 30 min at 96 h AEL, dissected after 24 h and co-labeled with Ase, E-cad and Repo. Glial cells were identified by Repo; Repo-negative cells in E-cad expressing cell streams were counted as progenitors.

To quantify the number of Hth- and Ey-positive cells relative to the p-IPC, $y\hspace{0.1em} hs\text{-}FLP^{122}; act>y^+>Gal4\ UAS\text{-}GFP\ dpp\text{-}lacZ/+; UAS\text{-}so\ UAS\text{-}eya/+$ larvae were heat shocked at 37°C for 30 min at 72 h AEL, dissected after 48 h and co-labeled with Hth and Fas3, and Ey and E-cad, respectively. Images were collected in horizontal orientation from three optical sections per sample (6- μm distance each). Cells were counted in $50 \mu\text{m}^2$ regions of interest with the lower edge aligned with the lower edge of the p-IPC.

Supplementary References

- Almeida, M. S. and Bray, S. J.** (2005). Regulation of post-embryonic neuroblasts by Drosophila Grainyhead. *Mech. Dev.* **122**, 1282-1293.
- Apitz, H. and Salecker, I.** (2015). A region-specific neurogenesis mode requires migratory progenitors in the Drosophila visual system. *Nat. Neurosci.* **18**, 46-55.
- Bazigou, E., Apitz, H., Johansson, J., Loren, C. E., Hirst, E. M., Chen, P. L., Palmer, R. H. and Salecker, I.** (2007). Anterograde Jelly belly and Alk receptor tyrosine kinase signaling mediates retinal axon targeting in Drosophila. *Cell* **128**, 961-975.
- Bellaiche, Y., Gho, M., Kaltschmidt, J. A., Brand, A. H. and Schweisguth, F.** (2001). Frizzled regulates localization of cell-fate determinants and mitotic spindle rotation during asymmetric cell division. *Nat. Cell Biol.* **3**, 50-57.
- Bier, E., Vaessin, H., Younger-Shepherd, S., Jan, L. Y. and Jan, Y. N.** (1992). *deadpan*, an essential pan-neural gene in Drosophila, encodes a helix-loop-helix protein similar to the hairy gene product. *Genes Dev.* **6**, 2137-2151.
- Brand, M., Jarman, A. P., Jan, L. Y. and Jan, Y. N.** (1993). *asense* is a Drosophila neural precursor gene and is capable of initiating sense organ formation. *Development* **119**, 1-17.
- Cheyette, B. N., Green, P. J., Martin, K., Garren, H., Hartenstein, V. and Zipursky, S. L.** (1994). The Drosophila sine oculis locus encodes a homeodomain-containing protein required for the development of the entire visual system. *Neuron* **12**, 977-996.
- Chotard, C., Leung, W. and Salecker, I.** (2005). glial cells missing and gcm2 cell autonomously regulate both glial and neuronal development in the visual system of Drosophila. *Neuron* **48**, 237-251.
- Garrity, P. A., Lee, C. H., Salecker, I., Robertson, H. C., Desai, C. J., Zinn, K. and Zipursky, S. L.** (1999). Retinal axon target selection in Drosophila is regulated by a receptor protein tyrosine phosphatase. *Neuron* **22**, 707-717.
- Gaytan de Ayala Alonso, A., Gutierrez, L., Fritsch, C., Papp, B., Beuchle, D. and Muller, J.** (2007). A genetic screen identifies novel polycomb group genes in Drosophila. *Genetics* **176**, 2099-2108.
- Ito, K., Awano, W., Suzuki, K., Hiromi, Y. and Yamamoto, D.** (1997). The Drosophila mushroom body is a quadruple structure of clonal units each of which contains a virtually identical set of neurones and glial cells. *Development* **124**, 761-771.
- Kosman, D., Small, S. and Reinitz, J.** (1998). Rapid preparation of a panel of polyclonal antibodies to Drosophila segmentation proteins. *Dev. Genes Evol.* **208**, 290-294.
- Lee, T. and Luo, L.** (1999). Mosaic analysis with a repressible cell marker for studies of gene function in neuronal morphogenesis. *Neuron* **22**, 451-461.
- Newsome, T. P., Asling, B. and Dickson, B. J.** (2000). Analysis of Drosophila photoreceptor axon guidance in eye-specific mosaics. *Development* **127**, 851-860.
- Noro, B., Culi, J., McKay, D. J., Zhang, W. and Mann, R. S.** (2006). Distinct functions of homeodomain-containing and homeodomain-less isoforms encoded by homothorax. *Genes Dev.* **20**, 1636-1650.
- Ohshiro, T., Yagami, T., Zhang, C. and Matsuzaki, F.** (2000). Role of cortical tumour-suppressor proteins in asymmetric division of Drosophila neuroblast. *Nature* **408**, 593-596.
- Pai, C. Y., Kuo, T. S., Jaw, T. J., Kurant, E., Chen, C. T., Bessarab, D. A., Salzberg, A. and Sun, Y. H.** (1998). The Homothorax homeoprotein activates the nuclear localization of another homeoprotein, extradenticle, and suppresses eye development in Drosophila. *Genes Dev.* **12**, 435-446.
- Patel, N. H., Snow, P. M. and Goodman, C. S.** (1987). Characterization and cloning of fasciclin III: a glycoprotein expressed on a subset of neurons and axon pathways in Drosophila. *Cell* **48**, 975-988.
- Pignoni, F., Hu, B., Zavitz, K. H., Xiao, J., Garrity, P. A. and Zipursky, S. L.** (1997). The eye-specification proteins So and Eya form a complex and regulate multiple steps in Drosophila eye development. *Cell* **91**, 881-891.

- Russell, S. R., Sanchez-Soriano, N., Wright, C. R. and Ashburner, M.** (1996). The Dichaete gene of *Drosophila melanogaster* encodes a SOX-domain protein required for embryonic segmentation. *Development* **122**, 3669-3676.
- Samakovlis, C., Hacohen, N., Manning, G., Sutherland, D. C., Guillemin, K. and Krasnow, M. A.** (1996). Development of the *Drosophila* tracheal system occurs by a series of morphologically distinct but genetically coupled branching events. *Development* **122**, 1395-1407.
- Spana, E. P. and Doe, C. Q.** (1995). The prospero transcription factor is asymmetrically localized to the cell cortex during neuroblast mitosis in *Drosophila*. *Development* **121**, 3187-3195.
- Struhl, G. and Basler, K.** (1993). Organizing activity of wingless protein in *Drosophila*. *Cell* **72**, 527-540.
- Tayler, T. D., Robichaux, M. B. and Garrity, P. A.** (2004). Compartmentalization of visual centers in the *Drosophila* brain requires Slit and Robo proteins. *Development* **131**, 5935-5945.
- Wodarz, A., Ramrath, A., Grimm, A. and Knust, E.** (2000). *Drosophila* atypical protein kinase C associates with Bazooka and controls polarity of epithelia and neuroblasts. *J. Cell Biol.* **150**, 1361-1374.